THE JOURNAL OF BIOLOGICAL CHEMISTRY VOL. 283, NO. 4, pp. 1902–1910, January 25, 2008

Ultra Short Yeast Tropomyosins Show Novel Myosin Regulation*

Received for publication, October 16, 2007, and in revised form, November 13, 2007 Published, JBC Papers in Press, November 14, 2007, DOI 10.1074/jbc.M708593200

Robin Maytum[‡1], Victoria Hatch[§], Manfred Konrad[¶], William Lehman[§], and Michael A. Geeves[‖]

From the [‡]School of Biological and Chemical Sciences, Queen Mary, University of London, E1 4NS, United Kingdom, the [¶]Max-Planck Institute for Biophysical Chemistry, Göttingen D-73070, Germany, the [§]Department Physiology & Biophysics, Boston University, Boston, Massachusetts 02118, and the [‖]Department of Biosciences, University of Kent, Canterbury CT2 7NJ, United Kingdom

Tropomyosin (Tm) is an α-helical coiled-coil actin-binding protein present in all eukaryotes from yeast to man. Its functional role has been best described in muscle regulation; however its much wider role in cytoskeletal actin regulation is still to be clarified. Isoforms vary in size from 284 or 248 amino acids in vertebrates, to 199 and 161 amino acids in yeast, spanning from 7 to 4 actin binding sites respectively. In *Saccharomyces cerevisiae*, the larger yTm1 protein is produced by an internal 38-amino acid duplication, corresponding to a single actin-binding site. We have produced an ultra-short Tm with only 125 amino acids by removing both of the 38 amino acid repeats from yTm1, with the addition of an Ala-Ser extension used to mimic the essential N-terminal acetylation. This short Tm, and an M1T mutant of it, bind to actin with a similar affinity to most Tms previously studied ($K_{50\%} \sim 0.5$ μM). However, an equilibrium fluorescence binding assay shows a much greater inhibition of myosin binding to actin than any previously studied Tm. Actin cosedimentation assays show this is caused by direct competition for binding to actin. The M1T mutant shows a reduced inhibition, probably due to weaker end-to-end interactions making it easier for myosin to displace Tm. All previously characterized Tms, although able to sterically block the myosin-binding site, are able to bind to actin along with myosin. By showing that Tm can compete directly with myosin for the same binding site these new Tms provide direct evidence for the steric blocking model.

Tropomyosin (Tm)[2] appears to be as ubiquitous as actin in eukaryotes (1–3). It is a dimeric protein forming an elongated α-helical coiled-coil (4, 5). It is an actin-associated protein, the dimeric units interacting end-to-end along actin filaments to form a continuous strand that wraps around the surface of the actin filament (6, 7). In this way it acts to stabilize actin filaments, as shown by the effect of knockouts of *TPM1* in yeast, which have a sickly phenotype due to loss of their actin stress fibers (8, 9). It has been shown to be an essential protein in yeast, with knockouts expressing no Tm being lethal (9). However Tm functions not just as a structural protein, but also a regulatory one. Its role is best understood in the regulation of muscle contraction, where it is directly involved in regulating the myosin-actin interaction (reviewed in Ref. 10). Its wider role in regulation of non-muscle actin filaments is less well understood, although it is becoming clear that it plays an important role in functional regulation of the cytoskeleton (11).

From its essential roles in cytoskeletal and muscle regulation it is clearly important to understand how Tm functions. Although structurally it appears like a simple rod-like molecule, higher vertebrates express a large diversity of Tm isoforms. Mammals express over 20 isoforms from four different genes (1). As highlighted in the skTm sequence shown in Fig. 1*A*, alternate splicing of the 9 exon mammalian tropomyosins is limited to 3 areas, the N and C termini and exon 6. A number of studies have been made on the effects of isoform and sequence changes in these regions, showing these areas to be significant in modulating Tm function (12–21). Fig. 1*A* also shows the decrease in Tm size from the higher eukaryote Tms, which have 284 residues or 248 residues (the shorter formed by exclusion of exon 2) and span 7 or 6 actins, to those from lower eukaryotes, which have 199 or 161 residues and span 5 or 4 actins. Thus size as well as sequence varies and is presumed to relate to Tm function.

The coiled-coil structure of Tm by itself necessitates a degree of repetitiveness within the sequence to allow it to fold and form a pair of correctly interacting helices. A heptad repeat (referred to from A to G) is necessary for formation of the coiled-coil. This constrains residues in the core A and D positions to generally be hydrophobic, while those in the adjacent E and G positions are often charged to allow hydrogen bonding (22, 23). It must also have a further higher order repeat to allow binding to multiple, identical, actin binding sites. Despite these constraints, Tms in higher animals lack any true sequence repeats within their structure, as shown by the dot-plot of human skeletal Tm shown in Fig. 1*B*. In contrast yeast Tms have an easily identifiable internal repeat of 38 residues (Fig. 1*C*) with the two *Saccharomyces cerevisiae* Tms differing in size by the number of these repeats. Yeast Tm1 is 199 residues with two repeats, while yTm2 is 161 residues and has only one copy of the sequence (8, 9). This provides a clearly identifiable actin binding repeat, which differs from those identified in the skeletal sequence by McLachlan and Stewart (24), where they constrained their repeats to multiples of the heptad repeat of either 35 or 42 residues.

A number of deletion studies have been made of mammalian

* This work was supported by Wellcome Trust Grant No. 055881 (to M. A. G.) and by National Institutes of Health grants HL36153 and HL86655 (to W. L.). The costs of publication of this article were defrayed in part by the payment of page charges. This article must therefore be hereby marked "*advertisement*" in accordance with 18 U.S.C. Section 1734 solely to indicate this fact.

[1] To whom correspondence should be addressed: School of Biological and Chemical Sciences, Queen Mary, University of London, UK. Tel.: 44-207-8827012; Fax: 44-208-9830973; E-mail: r.maytum@qmul.ac.uk.

[2] The abbreviations used are: Tm, tropomyosin; yTm, yeast tropomyosin; skTm, skeletal tropomyosin; S1, myosin subfragment 1; CD, circular dichroism; MOPS, 3-(*N*-morpholino)propanesulfonic acid; EM, electron microscopy.

tropomyosins to examine the significance of the core actin repeats (25–29). Previous to this study, the shortest functional Tm made by sequence deletions was a 4 actin-spanning Tm based on skTm, of similar size to the shortest yeast Tms (27, 28). The experimental data for these short vertebrate Tms indicated that they significantly inhibited myosin-actin interaction in comparison to the full-length Tm. This information was then used to support a regulatory model involving a conformational change in the actin filament following release of steric blocking (27). Models linking regulation to conformational changes on actin have also been proposed by others (30, 31).

In this study we have produced several yeast deletion mutants to further investigate the relationships between structure and function in Tms. Comparison of Fig. 1, *B* and *C* shows the significant advantage of using the yeast Tm sequence for deletion studies over the skeletal Tm previously used. There are no obvious sequence repeats within the skTm sequence, meaning that deletion studies have been based upon the pseudo-repeats identified by McLachlan and Stewart (24). However the yeast sequence has two highly conserved 38-residue repeats, which are the appropriate size to be actin-binding repeats. We therefore produced an ultra-short Tm by deletion of both of these sites, as shown in Fig. 1*A*. A family of proteins with varying N termini based on this deletion construct have been characterized in both biophysical and biochemical assays. Although the constructs are well behaved in terms of their binding to actin, they are anomalous in their regulation of the myosin-actin interaction. An explanation for the unexpected regulatory behavior and its implications in differentiating between steric-blocking and actin-based regulatory models are provided.

EXPERIMENTAL PROCEDURES

DNA Constructs—General recombinant DNA techniques were performed as described in Sambrook *et al.* (32) or as recommended by the supplier.

Yeast *TPM1* and *TPM2* clones were available in the pJC20 expression vector from previous work (12, 33). The new constructs were produced by PCR using Taq polymerase (Roche Applied Science) with suitable primers. The internal deletion was made by a 2-step PCR process in which 5′- and 3′-fragments with matching overlap extensions were first made and then combined together in a second reaction to produce the final product with the internal deletion. External primers were designed to match the N- and C- terminal coding regions and including NdeI and BamHI (underlined) subcloning sites, respectively, for insertion into pJC20. The sequences used for the external primers were as follows: 5′-GGG CCC ATA TGG ACA AAA TCA GAG AAA AGC TA (yTm1 5′-forward primer), 5′-GGA ATT CCA TAT GGC GAG CAT GGA CAA AAT CAG AGA AAA GC (TPM1(n2) 5′-forward primer), and 5′-CCC TTG GGA TCC TCA CAA GTT TTC CAG AGA TGC AGC (yTm1 3′-reverse primer), 5′-CCC TTG GGA TCC TCA GTT TTC CAG AGA TGC AGC (yTm1 L199 × 3′-reverse primer). PCR products were cut with NdeI and BamHI, ligated into pJC20, and transformed into the *Escherichia coli* strain XL1-Blue. The sequences for the primers used for the internal deletions were as follows 5′-CGC GGA TCC CTA GTT TTC CAG AGA TGC (TPM1 site1 R), 5′-GGA GCA AGA GTC TCA CCA CTT GCA GTC CAA CAA CG (TPM1 site1–4 F). The entire coding regions of the mutants were verified by sequencing (MWG-Biotech).

Protein Expression and Purification—For protein expression the purified plasmids were transformed into competent BL21(DE3) pLys cells and plated for colony isolation. Trial expressions were performed by inoculating single colonies from each into 1 ml of LB medium containing 100 mg/l ampicillin. These were induced with 0.4 mM isopropyl-1-thio-β-D-galactopyranoside at an $A_{600\,nm}$ of 0.6–1.0. Cells were then grown for 3 h at 37 °C and 0.125 ml samples harvested and SDS-PAGE used to check expression levels. Cultures showing good levels of expression were then used to seed 1-liter cultures for protein production.

Cultures were grown to late exponential phase and induced overnight with 0.4 mM isopropyl-1-thio-β-D-galactopyranoside at 30 °C. Cells were harvested by centrifugation at 5000 × *g*, resuspended in 60 ml of lysis buffer (20 mM Tris, pH 7.5, 100 mM NaCl, 2 mM EDTA, 1 mg/liter DNase, 1 mg/liter RNase) and lysed by sonication. The samples were then heat treated at 80 °C for 10 min, cooled, then spun at 10,000 × *g* to pellet-precipitated protein and cell debris. Soluble Tm was then isoelectric-precipitated from the supernatant at pH 4.5 by addition of 0.3 M HCl. The solution was then left at 4 °C for 15 min, and the precipitate pelleted by centrifugation at 10,000 × *g*. Dependent upon yield the pellet was then resuspended in 10–20 ml of buffer (10 mM phosphate, pH 7.0, 100 mM NaCl) and the pH readjusted to 7 after the pellet was dissolved. This was then further purified using a 5 ml of Amersham Biosciences HiTrap-Q column, eluted with a 150–400 mM NaCl gradient, the Tm eluting at around 200–250 mM salt. Fractions containing Tm, as shown by SDS-PAGE, were pooled and concentrated by isoelectric precipitation. Purity was checked by SDS-PAGE and comparison of 280/260 nm absorbance ratio. Protein concentrations were estimated using extinction coefficients $E^{1\%}$ of 6.0, 8.3, and 9.0 cm^{-1} for yTm1, yTm2, and yTm1Δ23 based clones, respectively, calculated from the sequences using AnTheProt (Gilbert Deleage, IBCP-CNRS).

Electrospray Mass Spectrometry—Protein molecular weight was determined by electrospray MS. For this, 10 μM stock samples were dialyzed overnight against 1 mM Tris, pH 7.0. These samples were then acidified by addition of formic acid to 1% v/v and methanol to 10% v/v. Samples were applied at flow rates of 3–5 μl/minute to a Finnegan Mat LCQ ion-trap MS. Mass accuracy for yTm samples is expected to be 2–3 Da (1/10,000). Predicted molecular weights for proteins were calculated using AnTheProt (Gilbert Deleage, IBCP-CNRS).

Other Proteins and Reagents—Myosin subfragment 1 (S1) was prepared by chymotryptic digestion of rabbit myosin, as described by Weeds and Taylor (34). Its molar concentration was calculated from absorbance measurement at 280 nm using an $E^{1\%}$ of 7.9 cm^{-1} and a molecular weight of 115,000 Da. Rabbit actin was purified by the method of Spudich & Watt (35). Its molar concentration was determined by its absorbance at 280 nm using an $E^{1\%}$ of 11.08 cm^{-1} and a molecular weight of 40,000 Da. The preparation of pyrene-labeled actin was as previously described (36). Phalloidin (Sigma) stabilized F-actin was made by incubating a solution of 10 μM pyrene-actin with 10

μM phalloidin overnight in experimental buffer (20 mM MOPS pH 7.0, 200 mM KCl, 5 mM $MgCl_2$) at 4 °C.

CD and Fluorescence Spectroscopy—Initial CD spectra were measured using 0.5 mg/ml samples of protein in 10 mM sodium phosphate pH 7.0, 0.5 M NaCl, 5 mM $MgCl_2$, 1 mM dithiothreitol in a Jasco 600 CD spectrophotometer from 190 to 250 nm using a 0.5 mm cell at 20 °C. For measurement of melting, the temperature was adjusted and allowed to equilibrate for at least 5 min at each temperature before recording a spectrum. Exact cell temperature was recorded using a platinum resistance thermocouple mounted against the cell surface. Melting plots were then produced from a cross section through the spectra at the 222 nm peak.

Fluorescence titrations were measured at 20 °C using a Perkin Elmer 50B spectrofluorimeter, exciting at 365 nm with a 10-nm bandwidth and measuring emission at 405 nm with a 15-nm bandwidth. A total working volume of 2 ml was used in a constantly stirred 10 × 10 mm cell. Autotitrations were made by the continuous addition up to 50 μl of a concentrated S1 stock solution using a Harvard Apparatus Syringe Infusion Pump 22 driving a 100-μl glass syringe (Hamilton) as described previously (37). Data were acquired over a period of 250 s, with data points being collected every 0.5 s, using an integration time of 0.45 s. Recorded data were corrected for the dilution effect (a maximum of 2.5%) before analysis. Buffer solutions for the titrations were syringe-filtered (0.22 μm) to reduce background noise in the stirred cell. Mixing and equilibration of the reaction in the cell were checked as detailed previously to ensure that the reaction was effectively at equilibrium on the time scale of the experiment (37).

Cosedimentation and Quantitative Electrophoresis—Cosedimentation assays were performed by mixing actin with tropomyosins at the concentrations specified in the standard assay buffer (20 mM MOPS pH 7.0, 200 mM KCl, 5 mM $MgCl_2$) in a total volume of 100 μl. These were then incubated at 20 °C for 20 min. The actin was then pelleted (along with any bound proteins) by centrifugation at 100,000 × *g* for 20 minutes (Beckmann TLA110). Equivalent samples of pellet and supernatant were then separated by SDS-PAGE.

SDS-PAGE was performed according to Laemmli (38) using 13.5% acrylamide gels and stained with Coomassie Blue G-250. Gel quantification was carried out using an Epson 4990 Photo scanner with transparency adapter attached to a computer. The scanner was calibrated using an Agfa Agfatrans (Agfa) density step tablet and scanned TIFF images were analyzed using the Image-PC program (Scion Corp. based upon NIH-Image).

Electron Microscopy and Helical Reconstruction—Tm (20 μM) was combined with F-actin (20 μM) at room temperature (~25 °C). After ~10 min of incubation the sample was diluted 40-fold and applied to carbon-coated electron microscope grids and negatively stained as previously described (39). Electron micrograph images of decorated filaments were recorded on a Philips CM120 electron microscope at ×60,000 magnification under low dose conditions (~12e^-/Å^2). Micrographs were digitized at a pixel size corresponding to 0.7 nm in the filaments. Well-stained regions of filaments were selected and straightened as before (40, 41). Helical reconstruction was carried out by standard methods (42–44) as previously described (6, 45).

RESULTS

Production and Expression of Recombinant Proteins—The clones of yeast *TPM1* and *TPM2* were available from previous work, both with and without sequence encoding the N-terminal Ala-Ser- extension commonly used to substitute for N-terminal acetylation in recombinant versions expressed in *E. coli* (12, 33). The DNA sequences for the genes actually encodes (Met)-Ala-Ser-, but the N-terminal Met is removed post-translationally to leave just the dipeptide extension on the yTm1n2 and yTm2n2 proteins (12, 33), as shown for other similar N-terminal sequences (16, 18). To simplify nomenclature in this article, henceforth all constructs will be assumed to have the dipeptide extension unless otherwise stated and will just be referred to as yTm1 and yTm2. The new constructs made for this work were based upon deletion of both of the 38-residue internal repeats found in the yTm1 sequence as shown in Fig. 1*A*. Three versions of this construct were planned, a native form without any extension, one with the Ala-Ser- extension and another based on the native form, but with the C-terminal residue deleted. The latter (ΔC) version was made to facilitate future crystallization trials, as it had been previously shown that deletion of the C-terminal Leu of native acetylated Tm prevented binding to actin (12). Sequencing of the clones showed all to have the correct sequence, apart from one of the two yTm1 clones sequenced, which contained a mutation of the first Met of the native sequence to Thr. This is an unusual mutation as it is within the primer sequence used for PCR and would be unlikely unless there is an error in the primer resulting in all clones containing the error. As this M1T mutation was within the N-terminal region that has been shown to have significant effects upon Tm regulatory properties (12, 33), protein was produced and characterized along with the other clones. Yields after purification were good for all clones (10–30 mg/liter cells), and within the range previously shown for yTm1 and yTm2 constructs (12, 33). The molecular mass of each purified protein was confirmed by electrospray mass spectrometry. Predicted masses are 14952.4, 14922.3, 14794.2, and 14681.1 for 1d23, 1d23M1T, 1d23-Ac, and 1d23ΔC, respectively. Determined masses were 14952.0, 14927.0, 14794.0, and 14681.0 corresponding within the expected error for these measurements.

Tropomyosin Binding to Actin—Initial qualitative binding studies of the constructs were done by adding an excess of each of the Tms (~3 μM) to 10 μM F-actin and quantifying bound and free Tm on a gel as detailed previously (12). The gel in Fig. 2 shows comparison of binding of yTm1, yTm2, and yTm1d23 constructs. Although not further included in this study, the inclusion of yTm2n2 allows comparison of 5, 4, and 3 actin-spanning Tms (~199, 161, and 123 residues, respectively) on a single gel. All of the yeast tropomyosin constructs run at higher than their expected weight on SDS-PAGE. The new yTm1d23 (referred to henceforth as 1d23) constructs run approximately halfway between the 14-kDa and 23-kDa markers, significantly higher than their <15-kDa size. The gel shows all the 1d23 constructs behaved as would be predicted from previous work (12, 33). The Ala-Ser- versions of the 1d23 and 1d23M1T con-

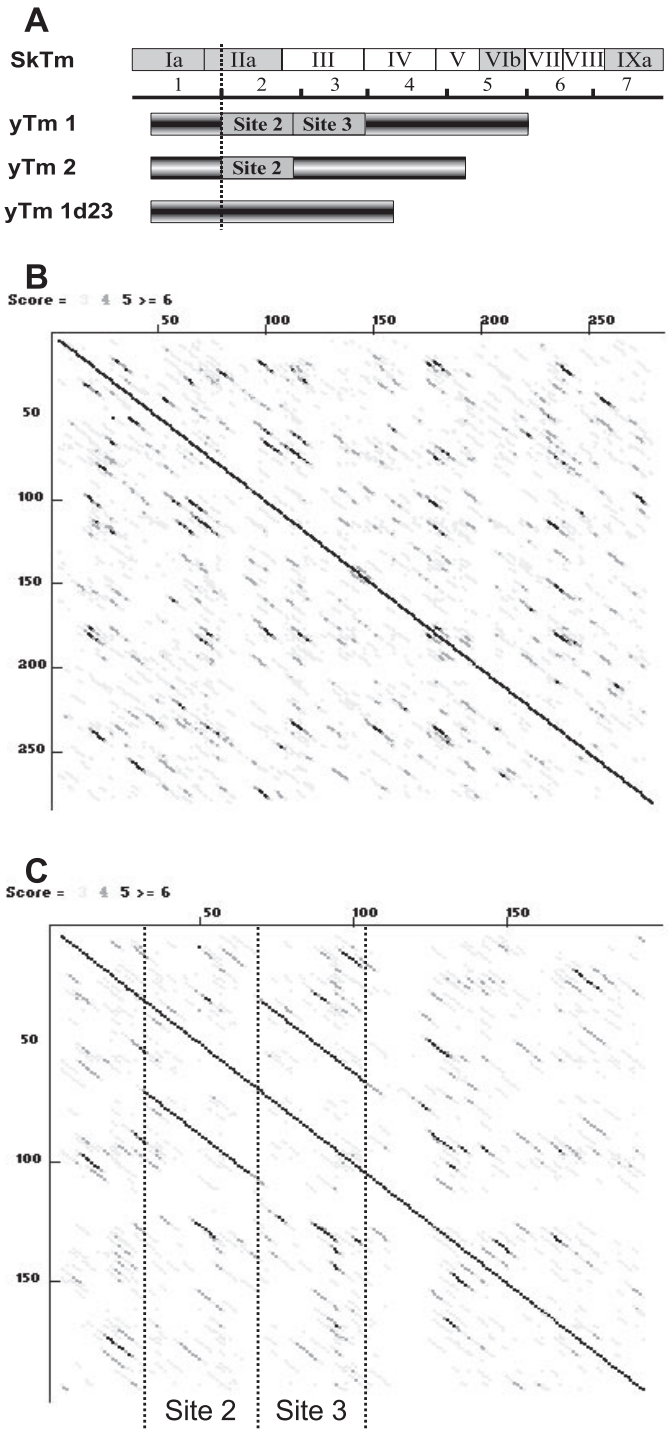

FIGURE 1. *Panel A* shows an alignment of mammalian skeletal tropomyosin with the two *S. cerevisiae* Tms, yTm1 and yTm2. The sequences are aligned *versus* the site 1-site 2 boundary of the seven actin pseudo-repeats of skTm identified by McLachlan and Stewart (shown below skTm). The sequences of the two yTms plus the novel Tm produced for this study are then shown below. The skTm sequence shows its 9 exon structure, with the alternatively spliced exons (1, 2, 6, and 9) shaded *gray*. The internal repeats of 38 residues within the yeast sequences, presumed to be an actin-binding repeat, are shown and used to define the site 1-site 2 boundary for these sequences. Panels *B* and *C* show dot-plots for the skTm and yTm1. The clear internal repeats identified by the dot-plot within yTm1, corresponding to sites 2 and 3, are highlighted in *C*.

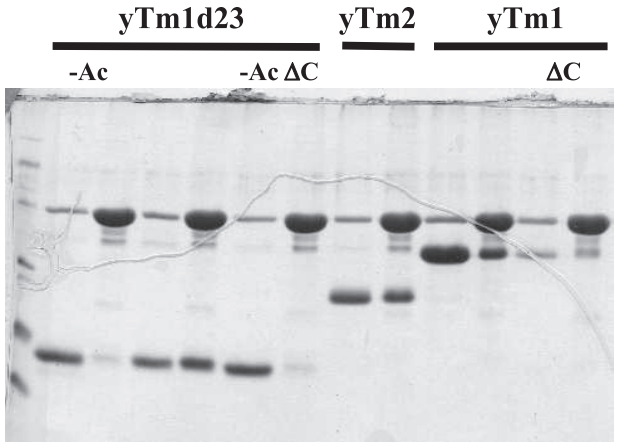

FIGURE 2. **Binding of the yeast Tm constructs used in this study to actin, determined by cosedimentation in 20 mM MOPS pH 7.0, 200 mM KCl, 5 mM $MgCl_2$.** An excess of tropomyosin was mixed with 10 μM actin and then cosedimented at 100,000 × *g* for 20 min. Equivalent samples of the supernatant (*left*) and pellet (*right*) for each sample were separated by SDS-PAGE. Constructs are labeled in combinations of: *-Ac*, having just the native sequence with no acetylation; *ΔC*, which have the C-terminal Leu residue removed; *-AcΔC*, which has both the deletion and no acetylation. All others have an additional Ala-Ser- on the N terminus.

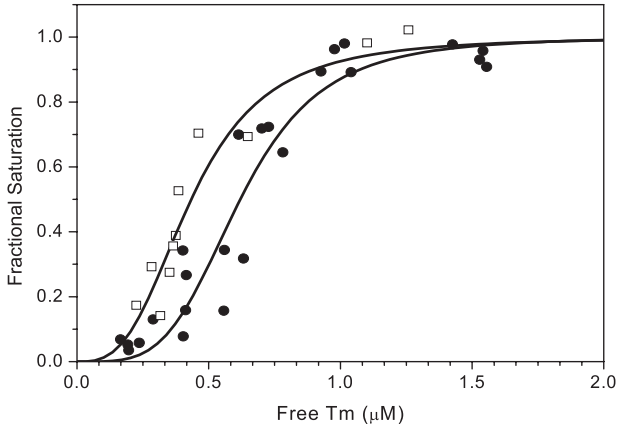

FIGURE 3. **Binding curves of 1d23 (*open squares*) and 1d23M1T (*filled circles*) to actin determined by cosedimentation of increasing concentrations of Tm (0.5, 1, 2, 3, 4, 5 μM) with 10 μM actin as described in the legend to Fig. 2.** After separation by SDS-PAGE the concentrations of free and bound tropomyosin were determined by quantitative scanning of the Coomassie blue-stained gels. For simplicity the *y*-axis is plotted as the staining ratio, the ratio of the absorbance of the Tm/actin bands in the pellet. Curve fits to the data using the Hill equation are shown as *solid lines*.

TABLE 1

Binding data of Tms to actin (data for skTm and yTm1 from Maytum *et al.* (33))

	$K_{50\%}$ (actin)	Hill coeff	Size (residues)	Stoichiometry (actins per Tm)
skTm	0.34 ± 0.02 (2001)	3.24 ± 0.4	284	7
yTm1	0.95 ± 0.04 (2001)	4.8 ± 1.0	201	5
1d23	0.44 ± 0.05	3.5 ± 1.0	125	3
1d23M1T	0.62 ± 0.04	4.0 ± 0.8	125	3

structs bind to actin with a similar affinity to that previously characterized for yTm1 and yTm2 (1d23M1T not shown in Fig. 2, but see Fig. 3 and Table 1). Also as expected there is no significant binding of either the unacetylated-Ac native or -AcΔC versions. The gel also shows however that an yTm1ΔC construct retains some binding affinity to actin.

Binding curves were then generated for the 1d23 and 1d23M1T Tms by quantitative analysis of gels from cosedimentations containing 0.2–4 μM Tm and are shown in Fig. 3. Both show the cooperative binding curves expected for Tms. Quan-

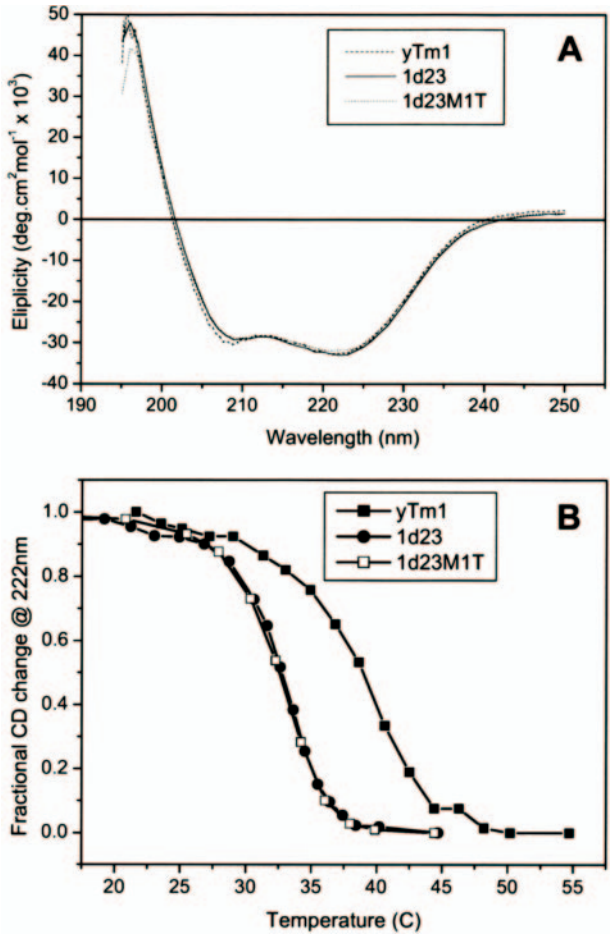

FIGURE 4. *Panel A*, comparison of CD spectra of Ala-Ser- versions of recombinant yTm1 plus the two deletion constructs 1d23 and 1d23M1T. Spectra were measured from 195–250 nm in 10 mM phosphate, pH 7.0, 500 mM KCl, 5 mM $MgCl_2$. *B*, CD melting curves for the same constructs measured at 222 nm. Melting curves are plotted as fraction of the total change in CD at 222 nm *versus* temperature.

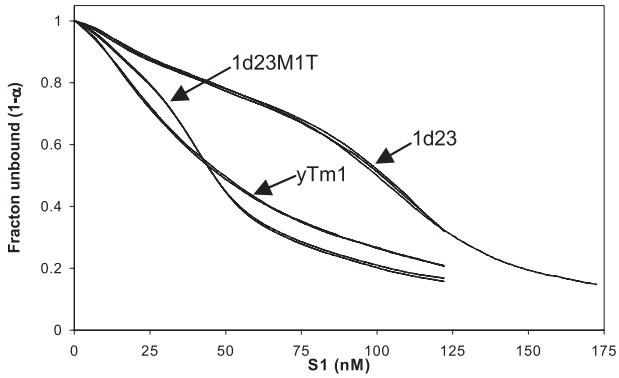

FIGURE 5. **Myosin S1 binding curves to 50 nM phalloidin stabilized pyrene-actin in the presence of 2 μM of each Tm, buffer conditions: 20 mM MOPS pH 7.0, 200 mM KCl, 5 mM $MgCl_2$.** Samples were allowed to equilibrate for 5 min before the addition of Myosin S1. Binding is plotted as fraction of free actin (without S1 bound) against S1 concentration. Replicates of either 2 or 3 experiments are shown for each Tm to demonstrate reproducibility.

tification shows they saturate at the same Tm/actin mass ratio seen for other Tms, confirming the expected 1:3 Tm:actin binding stoichiometry (see Table 1). The curve fits to the data show that the M1T mutation has a slightly lower affinity for actin (0.62 μM) than the native sequence (0.44 μM). Both of these affinities and the cooperativity of their curves (Hill coefficient) are in the same range as previously determined for the full-length yTm1 and skeletal Tm (see Table 1).

Circular Dichroism Melting Curves—Circular dichroism provides an effective measure of the folding of proteins. Spectra of the 1, 1d23 and 1d23M1T are shown in Fig. 4*A*. Studies were performed in a high salt buffer (10 mM $NaPO_4$ pH 7.0, 0.5 M NaCl) to prevent self-association of Tms. The spectra are virtually identical, showing characteristic 222- and 208-nm peaks of tropomyosins. This shows they have the same mean residue ellipticity with identical secondary structures and are all fully folded α-helical coiled-coils.

Fig. 4*B* shows the thermal dependence of the CD ellipticity at 222 nm. This shows the effects of the internal deletion and M1T mutation. Repeated melting curves were identical to the initial ones, showing melting was fully reversible, as found for other Tms. The melting curve for yTm1 is virtually identical to previously published results, with a mid point of ~38 °C (12). It can be seen that the internal deletion significantly reduces the stability of the tropomyosin, reducing the mid point by around 6 °C to ~32 °C for both 1d23 and 1d23M1T. The melting curves for these two proteins are virtually identical, showing the M1T mutation has no detectable effect on protein folding.

S1 Binding to Actin·Tm Complex—The binding of myosin S1 to regulated thin filaments was measured by equilibrium fluorescence titrations under similar conditions to those previously described (37). For these titrations an excess of Tm is added (2 μM) to ensure that the thin filaments are saturated with Tm throughout the titration. This is well above the determined $K_{50\%}$, for the yTm1, 1d23, and 1d23M1T Tms.

Titrations of myosin S1 against 50 nM pyrene-labeled actin in the presence of the three Tms are shown in Fig. 5. Raw data showed no significant difference in the starting fluorescence or the degree of quenching (approx 60%) for actin alone or actin in the presence of any of the Tms measured. This demonstrates the pyrenyl signal for myosin binding is not affected by the presence of these novel Tms. The binding curves are shown plotted as the fraction of unbound actin against total S1 concentration as for previously published works (12, 33, 37, 46). Two or three datasets are shown overlaid for each Tm, to show the reproducibility of the data. The titration containing yTm1, gave a sigmoid curve as for previously published results, and could be fitted to a 2-state version of the 3-state McKillop & Geeves model of regulation (12). Parameters for the fitting of the yTm1 were comparable to those previously published (12, 33).

The titration curves for both the 1d23 Tms show significantly greater inhibition of S1 binding to actin than has been previously measured for tropomyosins without the presence of troponin. In this cooperative system inhibition of binding results in increasing sigmoidicity of the curve, rather than a large change in $K_{50\%}$ (as shown in Maytum *et al.* (12)). For 1d23, which shows the greater inhibition of myosin binding, the inhibition of myosin binding (seen by the sigmoidicity) is greater even to that seen from a switched off filament in the presence of troponin and absence of calcium (compare Fig. 3 of Maytum *et al.* (37)). However it was not possible to produce a reasonable fit to the titrations for 1d23 and 1d23 M1T using this model. The

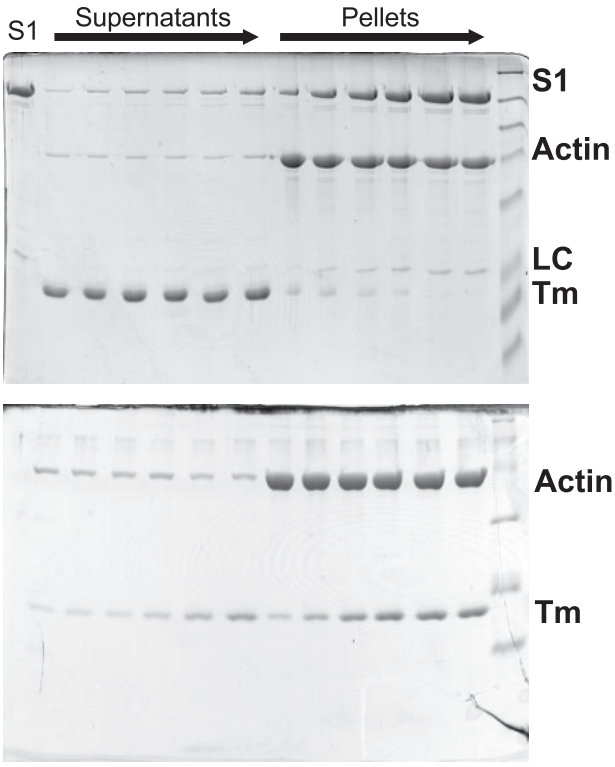

FIGURE 6. **Cosedimentation of 1d23 with actin in the presence (*top*) and absence (*bottom*) of an excess of myosin S1.** The gels show supernatants and pellets from cosedimentations containing 10 μM actin, myosin S1 (*top gel only*; 1, 2, 4, 6, 8, 10 μM *left to right*, labeled: *S1*, heavy chain; *LC*, light chains) and Tm (either 4 μM top, or 0.2, 0.5, 1, 2, 3, 4 μM increasing from left to right as *arrowed*, *bottom*). Buffer conditions are the same as for Fig. 2.

shapes of the binding curves are more complex than the sigmoidal curves measured for all previously studied tropomyosins, either on their own or in the presence of troponin (12, 33, 37, 46). This is best exemplified by the 1d23 curve in which two points of inflection can be seen, one at ~25 nM and another at ~110 nM. The 1d23 M1T construct shows a similar curve shape, although over a smaller concentration range meaning it is not quite so clearly resolved.

This curve shape corresponds to what would be expected from competitive stripping of Tm from actin according to the linear lattice models of Tm binding to actin proposed by Wegner (47) and Vilfan (48). This should produce the reverse of the cooperative binding curves seen in Fig. 3. However their models also predict a small proportion of sites without Tm bound giving that would produce a standard hyperbola superimposed on the sigmoidal unbinding curve, giving the inflection point seen. The first inflection was less noticeable in some batches of actin (data not shown). The relative midpoints of the unbinding curves (at ~50 nM and 110 nM S1 for 1d23M1T and 1d23) give values that differ to approximately the same degree as the binding curves (0.44 and 0.62 μM Tm, respectively).

Tropomyosin Binding to Actin in the Presence of Myosin S1—Fig. 6 shows the effect of myosin S1 upon the binding of 1d23 measured in a cosedimentation assay. An identical result was also found for the M1T mutant (not shown). It can be seen from the gel that as the concentration of myosin S1 present in the assay is increased, the amount of Tm bound to actin in the pellets decreases. All of the added Tm can be seen in the increasingly dense bands in the supernatants. This shows that Tm and S1 are binding competitively to the same site upon actin. This effect is unlike that observed for any previously characterized Tm. According to the steric blocking model and direct evidence from EM reconstructions, movement of Tm across the surface of actin normally allows both the myosin and Tm to bind simultaneously (45, 49, 50).

Electron Microscopy and Helical Reconstruction—Images of negatively stained thin-filaments were used to produce helical reconstructions of thin filaments containing 1d23. The results of this are shown in Fig. 7. The *top panel* shows the helical reconstruction of the actin-Tm filament at different contour levels. At the highest contour level (*right*) only the actin filament can be seen. As the contour level is reduced the Tm filament becomes visible and can be seen located on the inner domain of actin. The *bottom panel* shows a helical projection of the data, clearly showing location onto the inner domain of actin. This position is characteristic of the closed C-state of Tm upon actin (51).

DISCUSSION

In this study we have characterized the properties of yTm1d23 and a serendipitous mutant (M1T) that was produced. Using nature as a guide, deletion of both of the internal repeats within yTm1 has yielded an ultra-short Tm of only 123 residues. The recombinant versions of this Tm behave in a very similar manner to their larger relations. As can be seen in Fig. 1*A*, when the site 1–2 boundaries of yeast and skeletal Tms are aligned, the constraint of the McLachlan and Stewart actin-binding repeats to the heptad repeat means they do not align exactly with the subsequent yeast repeats. Their length-based calculation gave the repeat as 38 2/3 residues, which is however virtually the same size as sites 2 and 3 based on either system (42 + 35 in skTm *versus* 2 × 38 in yTm1). Likewise constraint of some of the previously made skTm deletions to whole heptads means they do not truly match an integer number of actin-binding sites. This will result in the Tm effectively being slightly over or under length. This is likely to effect end-to-end interactions, Tm filament compliance and hence regulatory properties as will be discussed later. This may explain some of the properties characterized for these constructs (25–29).

Fig. 2 shows the binding affinity of this construct to actin is very weak in the absence of the N-terminal Ala-Ser- extension necessary for most Tms to bind to actin in the absence of the native N-terminal acetylation (12, 16, 52). However with the addition of Ala-Ser- a tropomyosin is produced which binds to actin with an affinity around 0.5 μM, which seems common to the majority of all functional Tms from yeast to man (1, 2). The M1T mutation has a small effect on yTm1d23 affinity for actin (Fig. 3, Table 1), but the reduction in binding affinity is less than a factor of two. Circular dichroism (Fig. 4*A*) confirms the deletion constructs to be fully folded α-helical coiled-coils, as would be expected from their actin binding properties. CD melting data in Fig. 4*B* shows a significant reduction in the thermal stability of the deletion mutants, which is not unexpected as the deleted middle sections of Tm are generally more stable than the ends (53–55). Unlike some other small N-terminal sequence changes, the

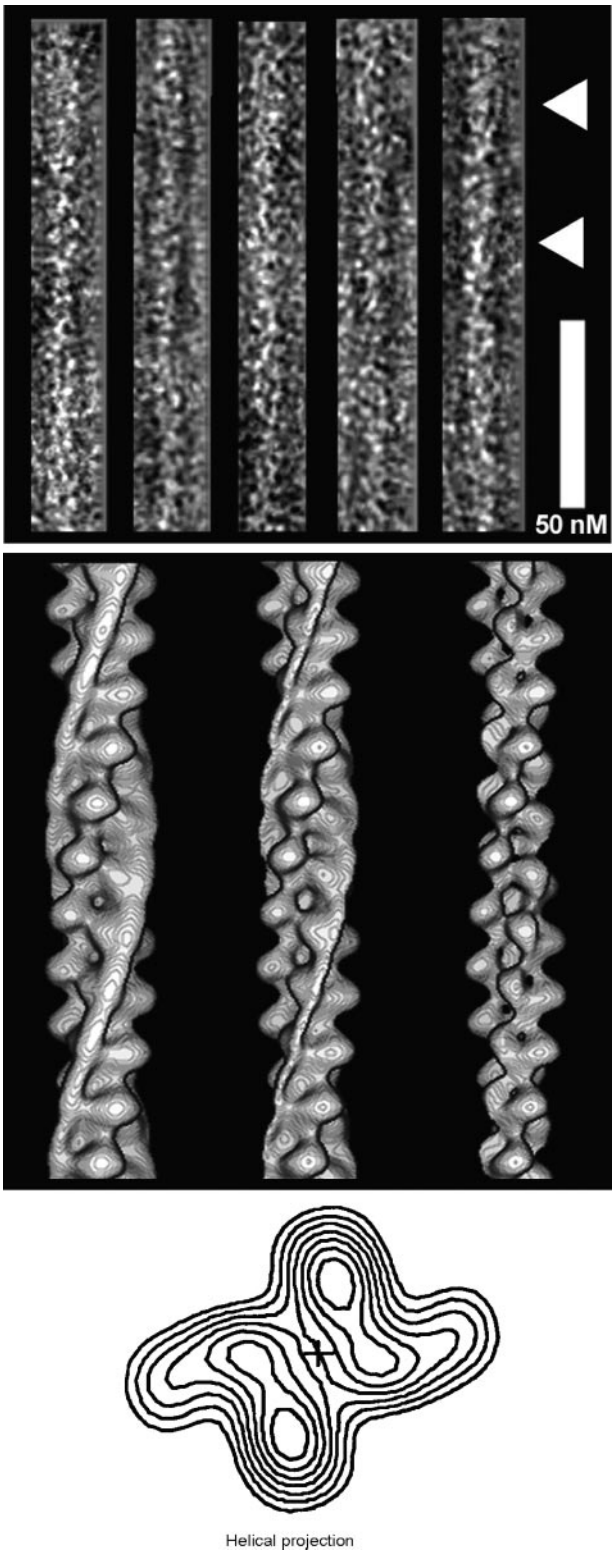

FIGURE 7. **Top shows raw negatively stained EM images of reconstituted actin-1d23 filaments.** *Arrows* show where Tm can be clearly seen on the rightmost filament. Middle shows helical reconstructions of 1d23 bound to actin produced from these EM images, shown at increasing contour threshold from left to right. *Bottom* is a helical projection derived from the data, showing a cross-section through the filament giving the location of the Tm strand relative to the actin filament.

M1T mutation does not have a measurable effect on the CD melting curve, as has been seen for yTm1 variants or for N-acetylation (12, 52).

According to all these criteria, the yTm1 deletion mutants are well-behaved Tms, shorter than any previously produced (27). However measurement of the regulation of myosin S1 binding showed binding curves that appeared somewhat anomalous, and it was not possible to fit them using the equations of the 3-state model (Fig. 5). This raised the possibility that the data would help to differentiate between a number of different models proposed for muscle regulation, which are all generally compatible with current data (37, 56–60). The models can be broadly classified into versions of the steric blocking model, where regulation is based upon a direct blocking of the myosin binding site by the position of Tm, and models for which the underlying mechanism is based upon an actin conformational change between forms for which myosin has a high and low affinity.

In fact, the cosedimentation data in the presence of an excess of myosin (Fig. 6) provides a clear, although unexpected, explanation that these short Tm constructs bind with myosin competitively. In striking contrast, vertebrate Tms bind cooperatively with myosin, showing a several order of magnitude increase in affinity. This has been proposed to support a regulatory model based upon a conformational change induced in the actin producing a high affinity myosin binding site (13, 14, 27, 61, 62). However, when yeast Tms are used in the same assays, measuring regulation of skeletal myosin binding to skeletal actin, they show good regulation without this huge increase in Tm affinity to acto-myosin (12, 33). This provides strong evidence that the reciprocal impact that Tm and myosin have on each other binding to actin is not necessarily fundamental to the mechanism of thin filament regulation. The yeast Tms bind in the same manner to actin as the vertebrate Tms with very similar affinities to actin (see Table 1 and Refs. 12, 33) and visualized by EM in the same position on actin as vertebrate Tms (Fig. 7, Ref. 51). There is no direct evidence for a change in the acto-myosin interaction in either case. As previously stated, the shape of the binding curves is nearly identical for full-length yeast constructs and vertebrate Tms. These can all be fitted equally well to the model with only the acto-myosin affinity differing (12, 33). All these data make it unlikely that yeast Tms display a fundamentally different type of regulation of the acto-myosin interaction. To fit this data in an actin-based regulatory model the high affinity actin state would need to have a variable affinity depending on the Tm present to be able to account for the previous yTm data and that shown here. The simpler explanation is the affinity changes are due to differing myosin-Tm interactions when myosin is bound, with the acto-myosin interaction remaining the same (33). This supports a direct steric blocking model of regulation with an unchanged acto-myosin interaction, but can it explain the competitive binding of myosin with Tm seen in this study?

The EM reconstructions of thin filaments shown in Fig. 7 show that the ultra-short Tms behave in a normal manner. The yeast Tm forms a strand that is clearly located into the closed C-position on the actin surface, which is most commonly occupied by Tms without the presence of other modifying proteins

(51). This C-position fits best with the predominant state determined thorough fitting of myosin binding data to the 3-state McKillop & Geeves model and this position may indicate a common minimum energy state for most Tms (12, 33, 37). These data show that the competitive binding of myosin and Tm to actin is not due to a novel or unusual binding mode of Tm to actin.

Putting the evidence together, the simplest explanation is consistent with steric-blocking theories of muscle regulation, where normally Tm forms a semi-flexible strand of end-to-end bonded molecules that blocks the myosin binding site on actin. The Tm strand can be considered like a guitar string on the surface of actin. It vibrates around an average, minimum energy, position on the surface, but can be constrained to either side by the binding of troponin or myosin. However, in the case of the deletion mutant studied here, the string is stretched more tightly. In this case its vibration is less likely to move far enough to allow myosin binding. However when it is trapped in the open M-state, which is increasingly likely as the myosin concentration is increased, it is forced to adopt a higher energy conformation. Lateral displacement from the minimum energy well will effectively stretch the tropomyosin, similar to sideways movement in our guitar string analogy. If the Tm strand has insufficient compliance to accommodate the stretch, then it will break at its weakest points, the end-to-end contacts. As Tm affinity for actin is due primarily to it forming a continuous strand wrapped around the actin helix, breaking the strand catastrophically reduces the binding affinity. This is demonstrated by the low affinity to actin of non-polymerizable Tms with weak end-to-end interactions (12, 19, 21, 52, 63), Hence with a taught strand, as with these ultra-short yeast Tms, binding of myosin and Tm therefore becomes competitive, as the Tm cannot accommodate the additional strain caused by displacement due to myosin binding. This interpretation is supported by the data for the M1T mutant. This shows a slightly lower binding affinity to actin, presumably due to the weaker end-to-end interactions caused by the change in N-terminal sequence. These weaker interactions are more easily broken, making the Tm more easily displaced by myosin as shown by the lower concentrations needed to displace it in the titrations in Fig. 5. The form of the unbinding curves fits well with predictions from the linear lattice binding models previous proposed for Tm to actin (47, 48). The variation in significance of the first inflection point between batches of actin matches the prediction of Vilfan that large filament sizes potentially produced *in vitro* would effectively increase the number of gaps present (48). Future work analyzing competitive binding at subsaturating concentrations and with treatments to vary actin filament size should allow further validation of these binding models.

This work therefore provides evidence supporting a direct steric-blocking model for regulation of the acto-myosin interaction. Steric-blocking can be understood in terms the semi-flexible filament theories proposed for Tm, in which Tm has persistence lengths of 7–14 actin monomers that have been used to explain a large amount of biochemical data on thin-filament regulation (37, 57, 64–66).

REFERENCES

1. Lees-Miller, J. P., and Helfman, D. M. (1991) *Bioessays* **13,** 429–437
2. Liu, H. P., and Bretscher, A. (1989) *Proc. Natl. Acad. Sci. U. S. A.* **86,** 90–93
3. Balasubramanian, M. K., Helfman, D. M., and Hemmingsen, S. M. (1992) *Nature* **360,** 84–87
4. Phillips, G. N., Jr., Lattman, E. E., Cummins, P., Lee, K. Y., and Cohen, C. (1979) *Nature* **278,** 413–417
5. Phillips, G. N., Jr., Fillers, J. P., and Cohen, C. (1986) *J. Mol. Biol.* **192,** 111–131
6. Vibert, P., Craig, R., and Lehman, W. (1993) *J. Cell Biol.* **123,** 313–321
7. Holmes, K. C., Tirion, M., Popp, D., Lorenz, M., Kabsch, W., and Milligan, R. A. (1993) *Adv. Exp. Med. Biol.* **332,** 15–22; discussion 22–14
8. Liu, H. P., and Bretscher, A. (1989) *Cell* **57,** 233–242
9. Drees, B., Brown, C., Barrell, B. G., and Bretscher, A. (1995) *J. Cell Biol.* **128,** 383–392
10. Gordon, A. M., Homsher, E., and Regnier, M. (2000) *Physiol. Rev.* **80,** 853–924
11. Gunning, P. W., Schevzov, G., Kee, A. J., and Hardeman, E. C. (2005) *Trends Cell Biol.* **15,** 333–341
12. Maytum, R., Geeves, M. A., and Konrad, M. (2000) *Biochemistry* **39,** 11913–11920
13. Moraczewska, J., and Hitchcock-DeGregori, S. E. (2000) *Biochemistry* **39,** 6891–6897
14. Moraczewska, J., Nicholson-Flynn, K., and Hitchcock-DeGregori, S. E. (1999) *Biochemistry* **38,** 15885–15892
15. Maytum, R., Schafer, F., and Geeves, M. A. (2003) *Biophys. J.* **84,** 319A
16. Monteiro, P. B., Lataro, R. C., Ferro, J. A., and Reinach, F. D. C. (1994) *J. Biol. Chem.* **269,** 10461–10466
17. Pittenger, M. F., and Helfman, D. M. (1992) *J. Cell Biol.* **118,** 841–858
18. Novy, R. E., Liu, L. F., Lin, C. S., Helfman, D. M., and Lin, J. J. (1993) *Biochim. Biophys. Acta* **1162,** 255–265
19. Hitchcock-DeGregori, S. E., and Heald, R. W. (1987) *J. Biol. Chem.* **262,** 9730–9735
20. Hammell, R. L., and Hitchcock-DeGregori, S. E. (1997) *J. Biol. Chem.* **272,** 22409–22416
21. Hammell, R. L., and Hitchcock-DeGregori, S. E. (1996) *J. Biol. Chem.* **271,** 4236–4242
22. Greenfield, N. J., and Hitchcock-DeGregori, S. E. (1995) *Biochemistry* **34,** 16797–16805
23. Wagschal, K., Tripet, B., and Hodges, R. S. (1999) *J. Mol. Biol.* **285,** 785–803
24. McLachlan, A. D., and Stewart, M. (1976) *J. Mol. Biol.* **103,** 271–298
25. Hitchcock-DeGregori, S. E., Song, Y., and Moraczewska, J. (2001) *Biochemistry* **40,** 2104–2112
26. Hitchcock-DeGregori, S. E., and An, Y. (1996) *J. Biol. Chem.* **271,** 3600–3603
27. Landis, C., Back, N., Homsher, E., and Tobacman, L. S. (1999) *J. Biol. Chem.* **274,** 31279–31285
28. Landis, C. A., Bobkova, A., Homsher, E., and Tobacman, L. S. (1997) *J. Biol. Chem.* **272,** 14051–14056
29. Hitchcock-DeGregori, S. E., and Varnell, T. A. (1990) *J. Mol. Biol.* **214,** 885–896
30. Chen, Y., Yan, B., Chalovich, J. M., and Brenner, B. (2001) *Biophys. J.* **80,** 2338–2349
31. Ansari, S., El-Mezgueldi, M., and Marston, S. (2003) *J. Muscle Res. Cell Motil.* **24,** 513–520
32. Sambrook, J., Fritsh, E., and Maniatis, T. (1989) *Molecular Cloning A Laboratory Manual*, 2nd Ed., Cold Spring Harbor Laboratory, Cold Spring Harbor, NY
33. Maytum, R., Konrad, M., Lehrer, S. S., and Geeves, M. A. (2001) *Biochemistry* **40,** 7334–7341
34. Weeds, A. G., and Taylor, R. S. (1975) *Nature* **257,** 54–56
35. Spudich, J. A., and Watt, S. (1971) *J. Biol. Chem.* **246,** 4866–4871
36. Criddle, A. H., Geeves, M. A., and Jeffries, T. (1985) *Biochem. J.* **232,** 343–349
37. Maytum, R., Lehrer, S. S., and Geeves, M. A. (1999) *Biochemistry* **38,** 1102–1110

38. Laemmli, U. (1970) *Nature* **227,** 680–685
39. Moody, C., Lehman, W., and Craig, R. (1990) *J. Muscle Res. Cell Motil.* **11,** 176–185
40. Hodgkinson, J. L., Marston, S. B., Craig, R., Vibert, P., and Lehman, W. (1997) *Biophys. J.* **72,** 2398–2404
41. Egelman, E. H. (1986) *Ultramicroscopy* **19,** 367–373
42. DeRosier, D. J., and Moore, P. B. (1970) *J. Mol. Biol.* **52,** 355–369
43. Amos, L. A., and Klug, A. (1975) *J. Mol. Biol.* **99,** 51–64
44. Owen, C. H., Morgan, D. G., and DeRosier, D. J. (1996) *J. Struct. Biol.* **116,** 167–175
45. Vibert, P., Craig, R., and Lehman, W. (1997) *J. Mol. Biol.* **266,** 8–14
46. Maytum, R., Westerdorf, B., Jaquet, K., and Geeves, M. A. (2003) *J. Biol. Chem.* **278,** 6696–6701
47. Wegner, A. (1979) *J. Mol. Biol.* **131,** 839–853
48. Vilfan, A. (2001) *Biophys. J.* **81,** 3146–3155
49. Huxley, H. E. (1972) *Cold Spring Harbor Symp. Quant. Biol.* **37,** 361–376
50. Haselgrove, J. C. (1972) *Cold Spring Harbor Symp. Quant. Biol.* **37,** 341–352
51. Lehman, W., Hatch, V., Korman, V., Rosol, M., Thomas, L., Maytum, R., Geeves, M. A., Van Eyk, J. E., Tobacman, L. S., and Craig, R. (2000) *J. Mol. Biol.* **302,** 593–606
52. Urbancikova, M., and Hitchcock-DeGregori, S. E. (1994) *J. Biol. Chem.* **269,** 24310–24315
53. Palm, T., Greenfield, N. J., and Hitchcock-DeGregori, S. E. (2003) *Biophys. J.* **84,** 3181–3189
54. Smith, L., Greenfield, N. J., and Hitchcock-DeGregori, S. E. (1999) *Biophys. J.* **76,** 400–408
55. Greenfield, N. J., and Hitchcock-DeGregori, S. E. (1993) *Protein Sci.* **2,** 1263–1273
56. Tobacman, L. S., and Butters, C. A. (2000) *J. Biol. Chem.* **275,** 27587–27593
57. McKillop, D. F., and Geeves, M. A. (1993) *Biophys. J.* **65,** 693–701
58. Squire, J. M., and Morris, E. P. (1998) *Faseb. J.* **12,** 761–771
59. Borovikov, Y. S., Avrova, S. V., Vikhoreva, N. N., Vikhorev, P. G., Ermakov, V. S., Copeland, O., and Marston, S. B. (2001) *Int. J. Biochem. Cell Biol.* **33,** 1151–1159
60. Resetar, A. M., Stephens, J. M., and Chalovich, J. M. (2002) *Biophys. J.* **83,** 1039–1049
61. Cassell, M., and Tobacman, L. S. (1996) *J. Biol. Chem.* **271,** 12867–12872
62. Eaton, B. L. (1976) *Science* **192,** 1337–1339
63. Heeley, D. H., Golosinska, K., and Smillie, L. B. (1987) *J. Biol. Chem.* **262,** 9971–9978
64. Smith, D. A., Maytum, R., and Geeves, M. A. (2003) *Biophys. J.* **84,** 3155–3167
65. Lehrer, S. S., Golitsina, N. L., and Geeves, M. A. (1997) *Biochemistry* **36,** 13449–13454
66. Smith, D. A., and Geeves, M. A. (2003) *Biophys. J.* **84,** 3168–3180